Article

Optical Properties of Silicon Clusters in the Presence of Water: A First Principles Theoretical Analysis

David Prendergast, Jeffrey C. Grossman, Andrew J. Williamson, Jean-Luc Fattebert, and Giulia Galli

J. Am. Chem. Soc., **2004**, 126 (42), 13827-13837 • DOI: 10.1021/ja048038p

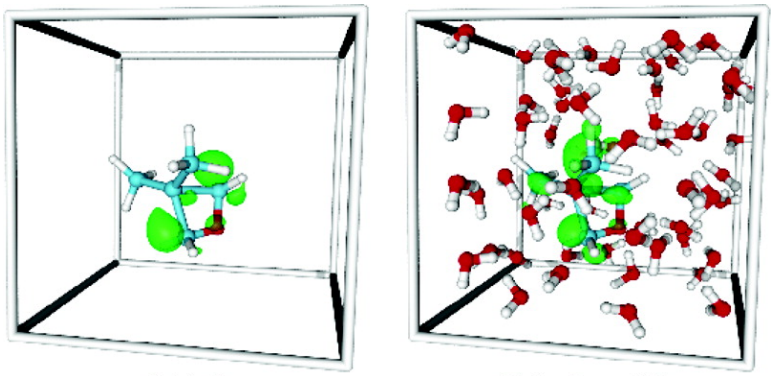

More About This Article

Additional resources and features associated with this article are available within the HTML version:

- Supporting Information
- Links to the 3 articles that cite this article, as of the time of this article download
- Access to high resolution figures
- Links to articles and content related to this article
- Copyright permission to reproduce figures and/or text from this article

View the Full Text HTML

J|A|C|S
ARTICLES
Published on Web 10/05/2004

Optical Properties of Silicon Clusters in the Presence of Water: A First Principles Theoretical Analysis

David Prendergast,* Jeffrey C. Grossman, Andrew J. Williamson, Jean-Luc Fattebert, and Giulia Galli

Contribution from the Lawrence Livermore National Laboratory, L-415, P.O. Box 808, Livermore, California 94551

Received April 5, 2004; E-mail: prendergast2@llnl.gov

Abstract: We investigate the impact of water on the optical absorption of prototypical silicon clusters. Our clusters contain 5 silicon atoms, tetrahedrally coordinated and passivated with either hydrogen or oxygen. We approach this complex problem by assessing the contributions of three factors: chemical reactivity, thermal equilibration, and dielectric screening. We find that the silanone (Si═O) functional group is not chemically stable in the presence of water and exclude this as a source of significant red shift in absorption in aqueous environments. We perform first principles molecular dynamics simulations of the solvation of a chemically stable, oxygenated silicon cluster with explicit water molecules at 300 K. We find a systematic 0.7 eV red shift in the absorption gap of this cluster, which we attribute to thermally induced fluctuations in the molecular structure. Surprisingly, we find no observable screening impact of the solvent, in contrast with consistent blue shifts observed for similarly sized organic molecules in polar solvents. The predicted red shift is expected to be significantly smaller for larger Si quantum dots produced experimentally, guaranteeing that their vacuum optical properties are preserved even in aqueous environments.

I. Introduction

Molecular sensing technology currently relies on fluorescent organic molecules as optical tags. However, these organic dyes have some deficiencies. They absorb light only at specific frequencies, making them inefficient emitters. Their optical emission cannot be tuned readily, and many molecules with unrelated structures and chemistry are required to produce a range of emission wavelengths. Furthermore, prolonged irradiation can lead to chemical or structural decomposition, altering or even destroying desirable optical properties during experiments. These deficiencies may be overcome by using semiconductor quantum dots (QDs) to develop new optical sensing technology.

QDs are pieces of bulk semiconductor in the nanometer-size regime. Their small size bestows them with optical properties that lie somewhere between those of molecules and those of the corresponding bulk materials. Like their bulk counterparts, QDs have robust atomic structures. They absorb light efficiently over a wide range of wavelengths, while emitting light of a characteristic frequency. In addition, due to quantum confinement effects, the optical properties of QDs may be tuned by controlling the size of each nanoparticle. These useful properties make QDs highly competitive with organic dyes for use as optical tags.

QDs made of silicon (Si) are highly desirable, given the abundance of this element and its use in the electronics industry. Also, in contrast with existing QD materials such as cadmium selenide (CdSe), porous silicon (one of the precursors of Si QDs) is both biostable and nontoxic.[1] Currently, the use of CdSe QDs as optical tags in biological environments requires coating with many layers of materials, to increase biostability and shield the biological environment from their inherent toxicity. Si QDs do not require any coating, and therefore the overall size of Si QDs is typically much smaller than that of coated CdSe QDs. This should permit the use of Si QDs, in aqueous environments,[2] to probe biochemical processes currently inaccessible to CdSe QDs − specifically processes which involve diffusion through intracellular membranes.

However, at present, Si QDs of a particular size, synthesized using different approaches, have a large distribution of measured optical properties, for example, photoluminescence from UV to red.[3] To shed light on the discrepancies between different experiments, first principles calculations have illustrated the important role of surface chemistry[4−10] and structure[11−15] on

(1) Mayne, A. H.; Bayliss, S. C.; Barr, P.; Tobin, M.; Buckberry, L. D. *Phys. Status Solidi A* **2000**, *182*, 505−513.
(2) Harwell, D. E.; Croney, J. C.; Qin, W.; Thornton, J. T.; Day, J. H.; Hajime, E. K.; Jameson, D. M. *Chem. Lett.* **2003**, *32*, 1194−1195.
(3) Wilcoxon, J. P.; Samara, G. A.; Provencio, P. N. *Phys. Rev. B* **1999**, *60*, 2704−2714.
(4) Filonov, A. B.; Ossicini, S.; Bassani, F.; d'Avitaya, F. A. *Phys. Rev. B* **2002**, *65*, 195317.
(5) Vasiliev, I.; Chelikowsky, J. R.; Martin, R. M. *Phys. Rev. B* **2002**, *65*, 123102.
(6) Puzder, A.; Williamson, A. J.; Grossman, J. C.; Galli, G. *Phys. Rev. Lett.* **2002**, *88*, 097401.
(7) Puzder, A.; Williamson, A. J.; Grossman, J. C.; Galli, G. *J. Chem. Phys.* **2002**, *117*, 6721−6729.
(8) Puzder, A.; Williamson, A. J.; Grossman, J. C.; Galli, G. *J. Am. Chem. Soc.* **2003**, *125*, 2786−2791.
(9) Zhou, Z. Y.; Brus, L.; Friesner, R. *Nano Lett.* **2003**, *3*, 163−167.
(10) Zhou, Z. Y.; Friesner, R. A.; Brus, L. *J. Am. Chem. Soc.* **2003**, *125*, 15599−15607.
(11) Weissker, H. C.; Furthmuller, J.; Bechstedt, F. *Phys. Rev. B* **2003**, *67*, 245304.
(12) Vasiliev, I.; Martin, R. M. *Phys. Status Solidi B* **2002**, *233*, 5−9.

the optical properties of Si QDs. From this body of work, it is now clear that the optical properties of Si QDs are not determined by size alone.

In this work, we analyze the impact of water on the optical absorption properties of Si nanoparticles. In the synthesis process or the application environment, water may be present, in vapor or liquid form, as a solvent or a contaminant. Furthermore, in applications to sensing in biological environments, water would be ubiquitous. Given the known impact of water − a polar solvent − on the absorption properties of solvated organic molecules, and the absence of equivalent information for inorganic solutes, analysis for Si nanoparticles in water is clearly necessary and important.

II. Consequences of Solute−Solvent Interaction for Optical Properties

In our study, we consider the solvation of an optically active species in a polar solvent. The strength of the solute−solvent interaction determines how much the optical properties of the total solvated system deviate from those of its constituents: the isolated solute and the solvent. If the electronic states involved in optical processes can be clearly associated with the solute (rather than with the solvent), then we may speak of the impact of the solvent on the solute, and that is the focus of this paper.[16] We consider three solute−solvent interactions contributing to changes in the optical properties of the solute: chemical reactivity, thermal equilibration, and dielectric screening.

Dielectric screening refers to the impact on the molecular and electronic structure of the solute due to screening of Coulomb interactions caused by the finite electrical susceptibilities of the solvent and solute. From the electrostatic point of view, this is a self-consistent phenomenon, where the charge density of the solute establishes a polarization of the solvent, which in turn impacts the solute charge density until some equilibrium is reached. Concomitantly, long-range electron correlation leads to attractive dispersion forces between the solute and solvent charge densities. The impact of these screening contributions on optical properties is explained in detail in section III, and the impact of screening on the Si clusters studied here is discussed in section X.

Sections IV and V contain details of our first principles calculations and the determination of excitation energies in solvated systems. Section VI outlines our understanding of Si clusters in vacuo, and in section VII we assess the impact of a solvation model on their structural and electronic properties. An investigation of the reactivity of various Si clusters with water is given in section VIII. Clearly, if the solute is chemically reactive in the presence of the solvent, the resulting reaction product may have a different molecular structure or composition and, consequently, a completely different optical signature.

Finally, in section IX, we examine the effect of thermally induced fluctuations in molecular structure on the optical properties of Si clusters. Thermal equilibration with a reservoir of solvent molecules will activate thermally accessible vibrational modes of the solute. Already, for Si clusters in vacuo at zero temperature, there is clear evidence of a large impact on the optical properties of these systems due to strain in the molecular structure, for example due to deviations from the preferred tetrahedral (sp^3) atomic coordination caused by surface relaxation.[11,13,14]

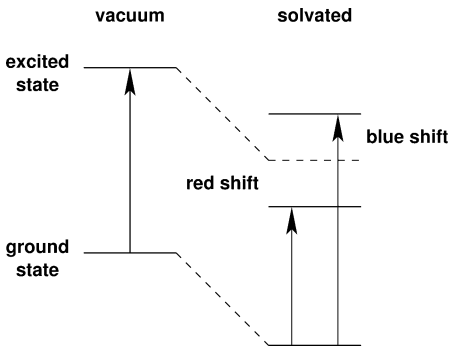

Figure 1. Schematic energy level diagrams for the electronic states involved in optical absorption for vacuum and solvated systems. Absorption energies required for transitions from ground to excited states are indicated with arrows. The solvation energy causes shifts in the total energy of the ground and excited states. The difference in solvation energies of the ground and excited states leads to a red or blue shift in the absorption energy with respect to the absorption energy in vacuo.

III. Solvent Screening and Optical Absorption

To study the impact of water on the optical absorption of Si nanoparticles, it suffices to assess the impact of solute−solvent interactions on the electronic ground state and on the first excited state. The solvation energy[17] may be different for ground and excited states, and this is the origin of so-called solvation shifts (Figure 1). If the solvation energy of the excited state is larger (smaller) than that of the ground state, we see a red (blue) shift in the absorption energy when compared to the unsolvated system.

One source of this difference in solvation energies is dielectric screening. For a large class of systems, probability distributions of excited state wave functions are more diffuse than those of the ground state, and consequently the system has a higher polarizability in the excited state than in the ground state. In general, the more polarizable is a system, the larger is its solvation energy. Therefore, if the excited state is screened by the solvent, this larger solvation energy will lead to a red shift in absorption. This is often the case for nonpolar solvents.

In polar solvents, a significant contribution to the screening comes from the alignment of molecular dipoles and occurs on the time scale of molecular motion. Upon absorption of a photon, there is not sufficient time for this orientational polarization to screen the resulting change in the electronic charge density of the solute. Hence, the resulting nonequilibrium excited state has a reduced solvation energy with respect to the ground state, leading to an overall blue shift in absorption (Figure 1).

In practice, both the fast and the slow components of the screening response of the solvent are present, leading to a net solvent shift. Water is a highly polar solvent, with an average

(13) Puzder, A.; Williamson, A. J.; Reboredo, F. A.; Galli, G. *Phys. Rev. Lett.* **2003**, *91*, 157405.
(14) Draeger, E. W.; Grossman, J. C.; Williamson, A. J.; Galli, G. *Phys. Rev. Lett.* **2003**, *90*, 167402.
(15) Draeger, E. W.; Grossman, J. C.; Williamson, A. J.; Galli, G. *J. Chem. Phys.* **2004**, *120*, 10807−10814.
(16) This picture is analogous to optically active point defects in solids, where defect states are introduced within the optical band gap of the solid, such that the optical properties of the combined system can be attributed to the defect rather than to the solid.
(17) The solvation energy is defined as [E(solute) + E(solvent)] − E(solute + solvent), where E(solute) is the total energy of the isolated solute; E(solvent) is the total energy of the pure solvent; and E(solute + solvent) is the total energy of the solvated system.

dipole moment per molecule of ~1.9 D in the gas phase. The electrical susceptibility of water can be separated into a static component χ_0 and an instantaneous component χ_∞ ($\chi_0 = \epsilon_0 - 1$, where ϵ_0 is the static dielectric constant, and $\chi_\infty = \epsilon_\infty - 1 = n^2 - 1$, where ϵ_∞ is the optical dielectric constant and n is the refractive index). For liquid water at room temperature, $\chi_\infty = 0.78$ and $\chi_0 \approx 77$. Experimental estimates of the Debye relaxation time for water provide an estimate of the time taken for reorganization of the orientational polarization in response to an external electric field. Current theories and experiments agree that there are two Debye relaxation times for water, one fast and one slow. The fast relaxation time has been tentatively associated with single molecular reorientation and has values from 0.2 to 1.5 ps at ambient conditions.[18,19] Therefore, we can assume that electronic absorption processes (occurring on 0.1 fs time scales) are instantaneous and that the excited states correspond to a nonequilibrium nuclear configuration. In addition, the large difference in magnitudes between χ_∞ and χ_0 increases the energetic cost of the excited state and generally leads to blue shifts in the absorption spectra of optically active polar organic molecules, for example, acetone (0.2 eV)[20] and pyridazine (0.5 eV).[21] In this paper, we will see (surprisingly) that these characteristic blue shifts are absent (or at least negligible in the presence of thermally induced structural fluctuations) for small inorganic Si clusters (see section X).

IV. First Principles Calculations

The optical properties of the various Si clusters examined in this paper are known to be particularly sensitive to their molecular structure.[13] Furthermore, the properties of the solvent and the nature of the solute−solvent interaction can be quite complex, involving charge-transfer, hydrogen-bonding, and long-range screening. To capture all of this in our theoretical approach, we need accurate descriptions of the electronic structure of these systems. For these reasons, we adopt first principles computational techniques, making use of density functional theory (DFT) within the generalized gradient approximation (GGA).

To simulate the impact of finite temperature and explicit solute−solvent molecular interactions, we use first principles molecular dynamics (FPMD), employing the Car−Parrinello method,[22] treating the nuclei in the system as classical particles acted upon by Coulombic interionic forces and quantum forces derived from the electronic structure.

The majority of electronic structure calculations in this paper were performed using the plane-wave pseudopotential codes GP[23] and ABINIT.[24] We also used the all electron code Gaussian 98.[25] FPMD simulations were carried out using GP. The DFT/GGA plane-wave pseudopotential calculations make use of the PBE exchange correlation functional[26] and use a basis of plane-waves consistent with periodic boundary conditions on a simulation box of a given size. The single-particle orbitals are expanded at the Γ-point only, for the valence electrons, with atomic cores represented by nonlocal, norm-conserving pseudopotentials.[27,28] The Gaussian-basis all electron calculations make use of the Becke functional[29] for exchange and the PW91 correlation functional.[30] These calculations are performed for finite systems using a 6-311G** Gaussian basis set.

A plane-wave kinetic energy cutoff of ~70 Ry[31] produces converged results for the electronic structure of the oxygen-containing Si clusters considered here and for water in the condensed phase. For calculations involving Si clusters in vacuo, simulation cell dimensions are chosen large enough to reduce the impact of finite size effects on the results. This is particularly important in calculations on small molecules where the spatial extent of unoccupied electronic states can be much larger than the atomic dimensions of the molecule.

As discussed in section III, to determine the absorption properties of a given system, we require explicit knowledge of the equilibrium electronic ground state and the nonequilibrium excited state. In practice, the absorption spectrum of a physical system is composed of many allowed electronic transitions and associated vibrational transitions. In this paper, we concentrate only on the lowest possible electronic transition in the absence of vibrational excitations. This marks the onset of optical absorption and is equivalent to the band gap of a solid-state system. We shall frequently refer to this energy as the absorption gap, E_g. In assessing the impact of water on the optical properties of Si clusters, we assume that a change in the absorption gap is indicative of an overall shift in the absorption spectrum of these systems.

Estimation of the absorption gap using first principles methods can be difficult. Electronic excitations are at heart many-body processes, and so are difficult to describe using effective single-particle DFT orbitals, especially because most correlation functionals are designed specifically for the electronic ground state. One common DFT estimate of E_g is the difference between the Kohn−Sham eigenvalues of the highest occupied molecular orbital (HOMO) and the lowest unoccupied molecular orbital (LUMO) of the ground-state electronic structure [Figure 2a]. For Si clusters in vacuo, this HOMO−LUMO gap has been shown to follow the same trends, as a function of size, as more accurate estimates of the absorption gap computed using quantum Monte Carlo (QMC) approaches or the *GW* approximation combined with a solution of the Bethe−Salpeter equation (*GW*- BSE).[32]

(18) Gaiduk, V. I. *Opt. Spectrosc.* **2003**, *94*, 199−208.
(19) Buchner, R.; Barthel, J.; Stauber, J. *Chem. Phys. Lett.* **1999**, *306*, 57−63.
(20) Bernasconi, L.; Sprik, M.; Hutter, J. *J. Chem. Phys.* **2003**, *119*, 12417−12431.
(21) Baba, H.; Goodman, L.; Valenti, P. C. *J. Am. Chem. Soc.* **1966**, *88*, 5410−5415.
(22) Car, R.; Parrinello, M. *Phys. Rev. Lett.* **1985**, *55*, 2471−2474.
(23) Gygi, F. *GP, a general ab initio molecular dynamics program*; Lawrence Livermore National Laboratory, Livermore, CA, 2003.
(24) Gonze, X.; Beuken, J.-M.; Caracas, R.; Detraux, F.; Fuchs, M.; Rignanese, G.-M.; Sindic, L.; Verstraete, M.; Zerah, G.; Jollet, F.; Torrent, M.; Roy, A.; Mikami, M.; Ghosez, P.; Raty, J.-Y.; Allan, D. *Comput. Mater. Sci.* **2002**, *25*, 478−492. The ABINIT code is a common project of the Université Catholique de Louvain, Corning Inc., and other contributors (URL http://www.abinit.org).
(25) Frisch, M. J.; Trucks, G. W.; Schlegel, H. B.; Scuseria, G. E.; Robb, M. A.; Cheeseman, J. R.; Zakrzewski, V. G.; Montgomery, J. A., Jr.; Stratmann, R. E.; Burant, J. C.; Dapprich, S.; Millam, J. M.; Daniels, A. D.; Kudin, K. N.; Strain, M. C.; Farkas, O.; Tomasi, J.; Barone, V.; Cossi, M.; Cammi, R.; Mennucci, B.; Pomelli, C.; Adamo, C.; Clifford, S.; Ochterski, J.; Petersson, G. A.; Ayala, P. Y.; Cui, Q.; Morokuma, K.; Malick, D. K.; Rabuck, A. D.; Raghavachari, K.; Foresman, J. B.; Cioslowski, J.; Ortiz, J. V.; Baboul, A. G.; Stefanov, B. B.; Liu, G.; Liashenko, A.; Piskorz, P.; Komaromi, I.; Gomperts, R.; Martin, R. L.; Fox, D. J.; Keith, T.; Al-Laham, M. A.; Peng, C. Y.; Nanayakkara, A.; Gonzalez, C.; Challacombe, M.; Gill, P. M. W.; Johnson, B.; Chen, W.; Wong, M. W.; Andres, J. L.; Gonzalez, C.; Head-Gordon, M.; Replogle, E. S.; Pople, J. A. *Gaussian 98*, revision A.7; Gaussian, Inc.: Pittsburgh, PA, 1998.
(26) Perdew, J. P.; Burke, K.; Ernzerhof, M. *Phys. Rev. Lett.* **1996**, *77*, 3865−3868.
(27) Hamann, D. R. *Phys. Rev. B* **1989**, *40*, 2980−2987.
(28) Troullier, N.; Martins, J. L. *Phys. Rev. B* **1991**, *43*, 1993−2006.
(29) Becke, A. D. *Phys. Rev. A* **1988**, *38*, 3098.
(30) Wang, Y.; Perdew, J. P. *Phys. Rev. B* **1991**, *43*, 8911−8916.
(31) In practice, we use a plane-wave cutoff of 69 Ry, which leads to more efficient grid dimensions for fast Fourier transforms.

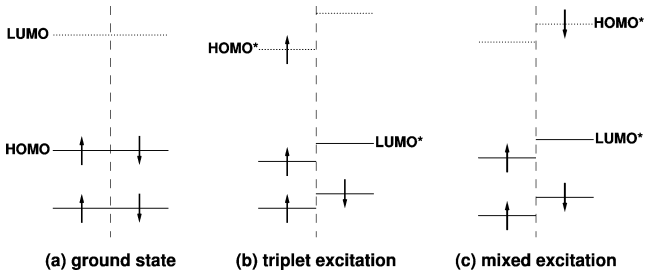

Figure 2. Schematic energy level diagrams of the electronic states considered in this paper, where single-particle orbitals are indicated by horizontal lines, energy increases in the vertical direction, and up and down spin channels are separated with a dashed line. (a) The spin degenerate ground state, indicating the highest occupied molecular orbital (HOMO) and the lowest unoccupied molecular orbital (LUMO). (b) The first excited state with triplet symmetry in a single reference picture, where the highest occupied (lowest unoccupied) molecular orbital of this excited-state configuration, labeled HOMO* (LUMO*), can be associated with the LUMO (HOMO) of the ground state. (c) The first excited state with mixed symmetry, with the HOMO* and LUMO* in the same spin channel.

To illustrate this point, we provide in section VI some QMC estimates of E_g for various silicon clusters containing 5 Si atoms but with different surface passivation. These QMC calculations were performed using the CASINO code.[33] The QMC trial wave functions are constructed using the standard Jastrow−Slater form.[34] The Jastrow correlation factor includes one- and two-body terms and is optimized using variance minimization.[35] A single Slater determinant is constructed using the Kohn−Sham orbitals of a ground-state DFT calculation (i.e., the same orbitals used to estimate the HOMO−LUMO gap). These orbitals are then transformed from the DFT plane-wave representation to a real-space maximally localized Wannier function representation to improve computational scaling in the evaluation of the Slater determinant.[36] The QMC Hamiltonian employs the same norm-conserving pseudopotentials as the DFT calculations. Following optimization of the Jastrow factor in a variational QMC calculation, we use the diffusion Monte Carlo method under the fixed-node-approximation to attain a more accurate estimate of total energy.[37]

We note, however, that the qualitative agreement in trends between gaps computed using DFT and QMC may be biased, given that the QMC trial wave functions are constructed from the same orbitals as those determined in the DFT calculation. This has been illustrated recently in an analysis of the excited states of ethene[38] and the photoisomerization of formaldehyde, formaldimine, and the protonated Schiff base.[39] In refs 38 and 39, QMC excited-state trial wave functions are expressed as a Jastrow correlation factor times a weighted sum of Slater determinants. The orbitals within this multiconfigurational wave function are optimized by minimization of the expectation value of the total energy, while maintaining orthogonality with the ground state. It was found that the trends in the excitation energy predicted by the restricted-open-shell Kohn−Sham (ROKS) approach[40] are not the same as those predicted by this more accurate QMC approach.

We have not performed such extensive QMC calculations in this work, but rely instead on the quantitative agreement between previous QMC estimates of E_g and estimates computed using the *GW-BSE* approach, previously obtained for isolated silicon clusters of comparable sizes to ours.[32] Furthermore, for solvated systems containing many explicit water molecules, the computational cost of performing QMC calculations of the gap is too great at present, and so we rely on DFT estimates. However, the approach we adopt to compute the gaps of these systems must go beyond the standard HOMO−LUMO estimate, if we wish to capture subtle solute−solvent interactions.

V. Calculation of Excitation Energies in the Presence of Solute−Solvent Interactions

The first excitation of a many-body ground state involves a transition to the next symmetry-allowed many-body eigenstate of the system's Hamiltonian. Clearly, this leads to a modified electronic charge density, which must be consistent with the dielectric properties of the solute and solvent. In an effective-single-particle theory such as DFT, the usual HOMO−LUMO gap is a poor estimate of this first excitation energy in the case of a solvated molecule. Apart from neglecting many-body effects due to the approximations involved in the exchange-correlation potential, there are more important electrostatic effects to consider. These include the relaxation of all of the single-particle orbitals in the presence of the charge density fluctuation due to the "electron−hole pair" created by the excitation. It is the screening of this fluctuation by the solvent that interests us as one of the possible impacts on the optical properties of the solute.

Therefore, to compute the excitation energies required to reach the first excited state, we adopt the delta-self-consistent-field (ΔSCF) approach.[41,42] This involves taking differences in total energy for two separate SCF calculations. We stress that this approach is adopted to better describe the physics of the solute−solvent interaction within the context of DFT (as outlined in section II). The importance of the ΔSCF estimator of E_g for solvated systems is discussed in section XI. To compute total energy differences, we make use of the following three total energies, each computed at a fixed molecular geometry:

(1) The ground-state energy is computed as usual with DFT. Each of the systems studied in this work is spin-symmetric in its ground state [Figure 2a]; therefore a spin-polarized calculation is not necessary, and the spatial parts of the Kohn−Sham eigenstates will be symmetric with respect to spin.

(2) The triplet first excited-state energy is computed in a spin-polarized calculation using the electron configuration outlined in Figure 2b. This spin-polarized state is the ground state for its spin symmetry. We impose no restriction on the Kohn−Sham eigenstates, which relax in the presence of the modified charge density, which includes a hole in the LUMO* and an electron in the HOMO* (states analogous to the HOMO and LUMO of the ground state, respectively). This total energy

(32) Williamson, A. J.; Grossman, J. C.; Hood, R. Q.; Puzder, A.; Galli, G. *Phys. Rev. Lett.* **2002**, *89*, 196803.
(33) Needs, R.; Towler, M.; Drummond, N.; Kent, P. *CASINO, version 1.7 User Manual*; University of Cambridge, Cambridge, 2004.
(34) Foulkes, W. M. C.; Mitas, L.; Needs, R.; Rajagopal, G. *Rev. Mod. Phys.* **2001**, *73*, 33−83.
(35) Umrigar, C. J.; Wilson, K. G.; Wilkins, J. W. *Phys. Rev. Lett.* **1988**, *60*, 1719−1722.
(36) Williamson, A.; Hood, R.; Grossman, J. *Phys. Rev. Lett.* **2001**, *87*, 246406.
(37) We use an imaginary time-step of 0.05 au for the diffusion Monte Carlo calculation.
(38) Schautz, F.; Filippi, C. *J. Chem. Phys.* **2004**, *120*, 10931−10941.
(39) Schautz, F.; Buda, F.; Filippi, C. 2004; Preprint: cond-mat/0404504.
(40) Frank, I.; Hutter, J.; Marx, D.; Parrinello, M. *J. Chem. Phys.* **1997**, *108*, 4060−4069.
(41) Gunnarsson, O.; Lundqvist, B. I. *Phys. Rev. B* **1976**, *13*, 4274−4298.
(42) Jones, R. O.; Gunnarsson, O. *Rev. Mod. Phys.* **1989**, *61*, 689−746.

includes the electrostatic attraction between the excited electron and the hole but also includes an exchange interaction between the two like-spin electrons nearest the Fermi level.

(3) A so-called mixed first excited state is computed using the electron configuration outlined in Figure 2c. While in the absence of any constraints this configuration would collapse to the ground state [Figure 2a], we prevent this by imposing two constraints on the SCF calculation. First, we constrain the occupations of states near the Fermi level such that the configuration of Figure 2c is maintained. This is equivalent to imposing that the z-component of the total electron spin is zero. We also then constrain all Kohn−Sham eigenstates of a given spin to be orthonormal. By insisting that the HOMO* is orthogonal to the LUMO*, we prevent this state from collapsing into the ground-state configuration. This approach leads to a single reference many-electron state of mixed spin-symmetry. With respect to the triplet state, the mixed state possesses a similar electrostatic interaction between the electron and hole; however, the exchange interaction present in the triplet case is now removed. In this sense, we draw a closer approximation to the true singlet. The numerical computation of the mixed state can be difficult given the inherent instability associated with the imposed constraints of occupancy and orthonormality. Therefore, we have performed mostly triplet excited-state calculations for the solvated systems and included some mixed-state calculations for comparison.

For the systems considered in this work, the first allowed electronic transition from the ground state is to a state with singlet symmetry. The representation of this singlet state requires more than one reference electron configuration. Because DFT is an effective single-particle method, we approximate this excitation with the single reference mixed state. This approximate singlet does not have the same symmetry as the true singlet, but it does contain a realistic approximation to the Coulomb interaction between the states near the Fermi level.

This mixed state has been employed in the past to approximate allowed first excitations in condensed matter, and also to extract the exchange splitting between light and dark excitons in semiconductors.[43] Exchange splittings determined using the mixed state typically underestimate the experimentally determined splitting. One may draw an analogy to Ziegler's sum method[44,45] for restricted Hartree−Fock eigenstates and approximate the singlet energy by using the relation: $E(\text{singlet}) = 2E(\text{mixed}) - E(\text{triplet})$. Approaches such as this have been adopted within the framework of DFT by restricting the spin-symmetry of all doubly occupied orbitals.[40,46] Unfortunately, when performing unrestricted DFT calculations for the excited configurations, this relation does not hold and thus has not been used here. However, we note that our mixed-state energies most likely underestimate the first singlet excited-state energy by an amount of the same order of magnitude as our estimate of the exchange splitting (see section XI).

VI. Silicon Clusters in the Absence of Water

The Si clusters studied in this paper are presented in Figure 3, and the corresponding estimates of the absorption gaps in vacuo are presented in Table 1. Despite definite inadequacy in the DFT estimates of the absorption gap, when compared to accurate QMC calculations, there are still consistent trends in comparison of the gaps of Si_5 clusters with different passivants. This has also been demonstrated in previous work over a wide range of Si cluster sizes.[6] Also, the smaller systematic differences between the two sets of DFT gaps, shown in Table 1, are due to the choice of exchange correlation functional and whether

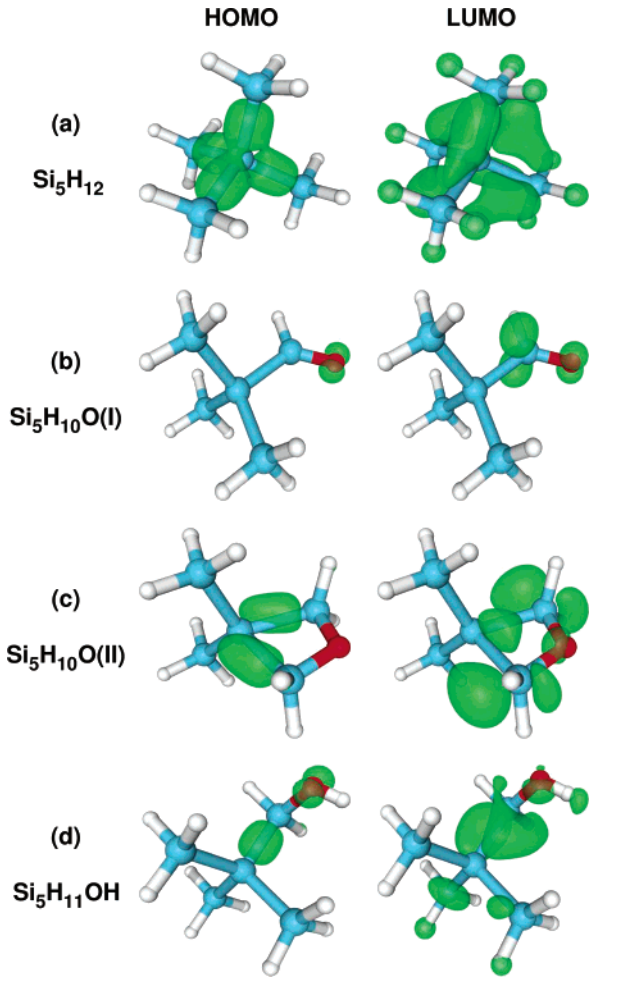

Figure 3. Structures of various silicon clusters and corresponding probability distributions (green) of the highest occupied molecular orbital (HOMO) and lowest unoccupied molecular orbital (LUMO). All electron density isosurfaces contain 30% of the total charge of the given state. Si atoms are colored blue, O atoms are red, and H atoms are white.

Table 1. Absorption Gaps (eV) and Dipole Moments (debye) for Various Silicon Clusters[a]

	E_g			dipole		
cluster	PBE-pp	PW91-ae	QMC	d_{vac}	d_{solv}	q
Si_5H_{12}	5.8	6.0	6.8	0.0	0.0	0.0°
$Si_5H_{10}O(I)$	2.9	3.1	3.6	4.5	6.2	8.5°
$Si_5H_{10}O(II)$	4.5	4.9	5.2	1.6	2.5	3.1°
$Si_5H_{11}OH$	4.7	5.0	5.4	1.2	2.0	4.9°

[a] Gaps estimated using: HOMO−LUMO DFT/PBE pseudopotential calculations (PBE-pp); HOMO−LUMO DFT/PW91 Gaussian basis set, all-electron calculations (PW91-ae); and QMC calculations (QMC) as described in the text. Dipole moments estimated from PBE-pp charge densities (d_{vac}). Also shown are dipole moments calculated in the presence of a continuum dielectric solvation model for water (d_{solv}) and the angular change in direction (θ) from the unsolvated dipole moment. (The symmetry of Si_5H_{12} guarantees that its dipole moment is zero.)

(43) Weissker, H.-C.; Furthmüller, J.; Bechstedt, F. *Phys. Rev. B* **2004**, *69*, 115310.
(44) Ziegler, T.; Rauk, A.; Baerends, E. J. *Theor. Chim. Acta* **1977**, *43*, 261−271.
(45) Daul, C. *Int. J. Quantum Chem.* **1994**, *52*, 867−877.
(46) Gräfenstein, J.; Kraka, E.; Cremer, D. *Chem. Phys. Lett.* **1998**, *288*, 593−602.

the pseudopotential approximation is adopted.[47] In our discussion below, we exploit the consistent trends in these calculated gaps, which allow qualitative comparison of the gaps of different systems as long as they are computed using the same level of theory.

Our reference structure is the "pure" hydrogen-saturated Si_5H_{12} [Figure 3a]. We also consider various types of surface passivation containing oxygen. The first, $Si_5H_{10}O(I)$, contains a silanone (Si═O) group [Figure 3b]. The departure from the local tetrahedral symmetry of each Si atom to a planar sp^2 symmetry for the SiHO portion of the molecule produces a localized HOMO and LUMO on this functional group. The localization effectively creates a defect state within the "band gap" of the molecule, reducing the absorption gap by almost 50%. We refer to previous work for a discussion of this effect for Si clusters of various sizes.[6]

We next consider two other forms of oxygen passivation that maintain, to a greater degree, the local tetrahedral symmetry of the Si atoms in the cluster. $Si_5H_{10}O(II)$ contains a bridging oxygen atom between neighboring Si atoms at the surface [Figure 3c]. This causes some strain in the angle between the surface Si atoms bonded to the O and the core Si atom, further reducing the tetrahedral angle from the ideal value (109.5°) to 70.4°. However, the preservation of approximate tetrahedral symmetry around each Si atom prevents the same degree of localization of the HOMO and LUMO as we see in $Si_5H_{10}O(I)$. Consequently, the impact of oxygen passivation on the absorption gap is diminished, and, for $Si_5H_{10}O(II)$, E_g is 25% less than that of Si_5H_{12}. $Si_5H_{11}OH$ contains a hydroxyl (OH) passivant, which has a reduced impact on the molecular structure in terms of strain, in comparison to $Si_5H_{10}O(I)$. However, there is still a reduction in the absorption gap due to the electronegativity of the O atom, which attempts to localize the states near the Fermi level around it [Figure 3d].

VII. Impact of a Continuum Solvation Model on Silicon Clusters

In a first approximation to the impact of water on the structure of these Si_5 clusters, we use a continuum solvation model[48,49] to simulate the electrostatic impact of the solvent. In this model, the explicit solvent molecules are replaced with a continuous scalar field which is designed to mimic the electrical permittivity of the water. This field is also a functional of the electronic charge density of the solute, that is, $\epsilon[\rho](r)$. The model ensures that ϵ attains the value of the bulk dielectric constant for water ($\epsilon_0 \approx 78$) in regions of space where ρ is effectively zero and smoothly decays to a value of unity for regions where ρ is significant. The parameters of the model control the rate of this decay to the vacuum permittivity and are fit to reproduce the solvation energy of a single water molecule.

We find almost no change in the atomic structure of these molecules in the presence of this solvation model. The most noticeable change is a 1% increase in the bond length of the silanone group in $Si_5H_{10}O(I)$. However, an examination of the impact of this solvation model on the dipole moments of each molecule indicates a consistent tendency to increase the dipole moment (Table 1). Given that the atomic structure remains unperturbed in the presence of the solvent polarization, this indicates that the increase in the dipole moment is caused by polarization of the electron charge density.

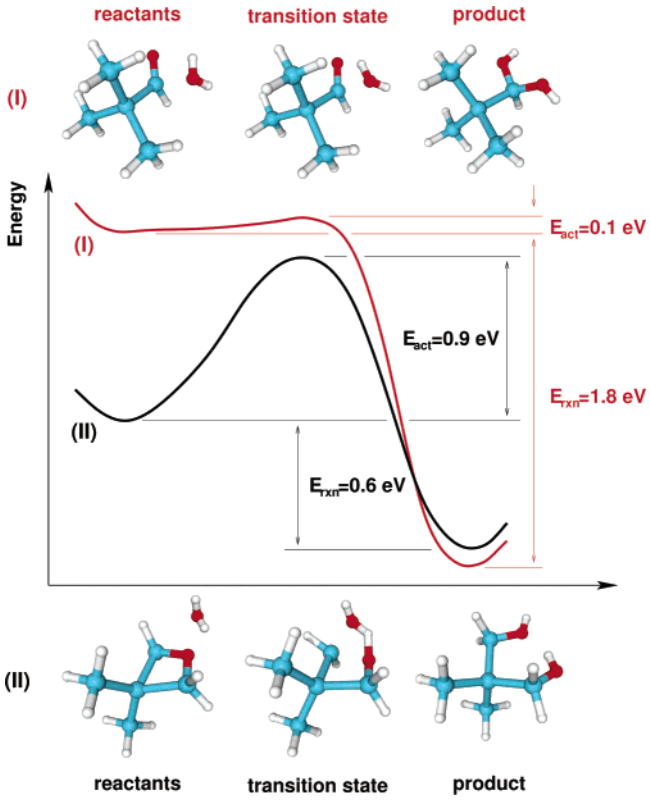

Figure 4. Reaction paths of $Si_5H_{10}O(I)$ (red) and $Si_5H_{10}O(II)$ (black) with one water molecule, indicating the activation energy E_{act} and the overall energy of reaction E_{rxn}.

VIII. Reactivity of Oxygenated Silicon Clusters with Water

The most striking impact of the solvent on a solute would be a chemical reaction producing a more stable chemical species, which we could expect to have optical properties quite different from those of its precursor. Of the four clusters considered in section VI, $Si_5H_{10}O(I)$ readily reacts with water to produce a dihydroxide according to the reaction:

$$Si_5H_{10}O(I) + H_2O \rightleftharpoons Si_5H_{10}(OH)_2 \qquad (1)$$

Using Gaussian 98, we determined a 0.1 eV activation energy for this reaction. This involved finding the total energy of the transition state for the reaction, by structural optimization in the direction of the eigenvector of the Hessian matrix with lowest negative eigenvalue. This reaction profile is compared, in Figure 4, to the same reaction for the stoichiometrically equivalent bridging structure $Si_5H_{10}O(II)$, which has a larger activation energy of 0.9 eV. This analysis indicates that the survival of silanone groups in water is highly unlikely, given the comparable size of the activation energy with the thermal energy at 300 K (i.e., ~0.03 eV). Also, this reaction is exothermic, and the energy released (~1.8 eV) would fuel the breakdown of other silanone groups by water.

(47) For example, we find a HOMO−LUMO gap of 5.9 eV for Si_5H_{12} in an all-electron calculation using the PBE exchange correlation functional. Introducing the pseudopotential approximation while retaining PBE leads to a gap of 5.8 eV (as shown in Table 1). Therefore, the pseudopotential approximation has a similar impact (~0.1 eV) on the HOMO−LUMO gap of these Si_5 clusters as a change in the type of GGA functional from PBE to PW91.

(48) Fattebert, J.-L.; Gygi, F. *J. Comput. Chem.* **2002**, *23*, 662.
(49) Fattebert, J.-L.; Gygi, F. *Int. J. Quantum Chem.* **2003**, *93*, 139.

Table 2. Variations in the HOMO−LUMO Gap (eV) during the Reaction with One Water Molecule for $Si_5H_{10}O$(I) and -(II) (Calculated Using PW91-ae)

cluster	reactants	transition state	product
$Si_5H_{10}O$(I)	3.8	4.0	5.3
$Si_5H_{10}O$(II)	4.7	4.1	4.7

Previous work by Zhou and Head[50] indicates a larger activation energy of 0.3 eV for the silanone group's reaction with water. However, the level of theory (MP2) and smaller system size (one Si atom) in that work may lead to a larger activation energy than the one found here. Furthermore, the 1% increase in the Si═O bond length in the presence of a polarizable solvent model (section VI) indicates that in liquid water this activation energy may be further reduced due to polarization of the $Si_5H_{10}O$(I) molecule and weakening of the Si═O bond. A recent study of the reactivity of several silica clusters with water by Laurence and Hillier,[51] using the B3LYP functional and a comparable basis to ours, reports activation energies of ~0.9 eV for the reaction of the Si−O−Si group with water, in good agreement with our result for the reaction of $Si_5H_{10}O$(II) with a water molecule.[52]

The reaction of $Si_5H_{10}O$(I) with water leads to a product with a larger absorption gap (Table 2). The restoration of the local sp^3 symmetry around the Si atom of the Si═O group relaxes the strain on the electronic structure, and the localized states present in the reactant disappear. This increases the DFT HOMO−LUMO gap from 3.8 eV (in the presence of a water molecule) to 5.3 eV, comparable to that of the single hydroxide.

We have also observed this reaction to take place in the course of a FPMD simulation of $Si_5H_{10}O$(I) in a simulation cell containing 57 water molecules. This reaction occurred while the system temperature was being equilibrated to 300 K, within the first 0.2 ps of the simulation. Therefore, we exclude this cluster from further tests on absorption in the presence of water. Given that the product of this reaction is a hydroxide, which is, energetically, significantly more stable than the silanone, we expect the hydroxide cluster to be a chemically stable species in water.

The absorption gap of $Si_5H_{10}O$(II) remains essentially the same at 4.7 eV, following the reaction with water. We regard this bridged cluster as chemically stable given its larger activation energy (0.9 eV) and smaller exothermic energy (0.6 eV) in comparison with that of the silanone cluster. Furthermore, as we see in section IX, during a 4.5 ps FPMD simulation, we do not observe the hydroxylation of this molecule when solvated in liquid water, despite large fluctuations in the cluster's average kinetic energy which were equivalent to temperatures exceeding 1000 K [Figure 5a].

IX. Impact of Finite Temperature on Optical Properties of Silicon Clusters

We simulate the solvation of the molecule $Si_5H_{10}O$(II) in water using FPMD. The simulation cell dimensions are (12.169 Å × 12.169 Å × 12.169 Å), and the cell contains 57 water molecules in addition to the solute. These cell dimensions were optimized to produce ambient pressure conditions using a classical MD simulation. The final configuration of this classical simulation was used as the starting point of the FPMD run.

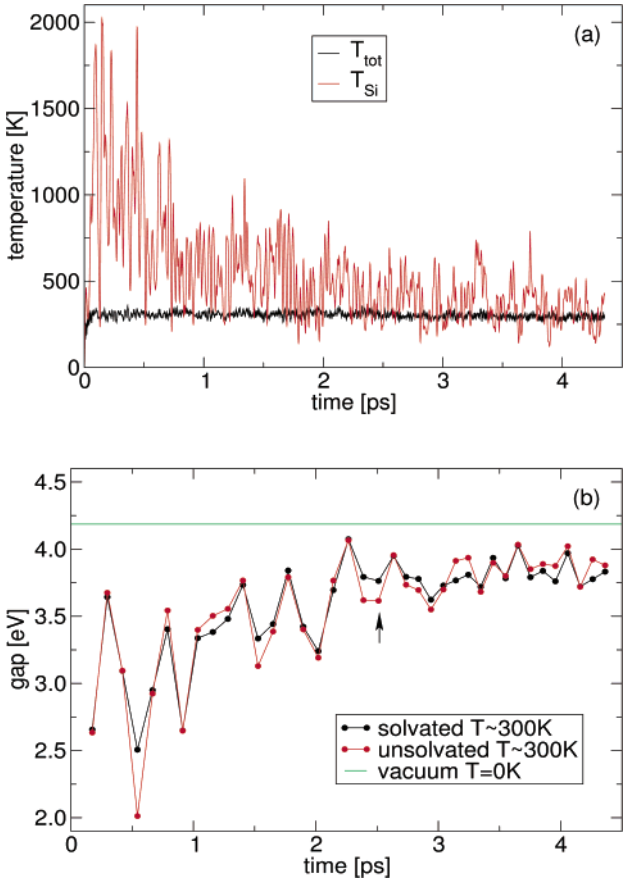

Figure 5. (a) System temperature T_{tot} (black) and the instantaneous average kinetic energy (converted to units of temperature) of the Si atoms T_{Si} as a function of time during an FPMD simulation of $Si_5H_{10}O$(II) in water. (b) The absorption gap of the solvated system (Si cluster and water molecules) computed at the indicated times during the course of the FPMD simulation (black) and the corresponding gap of the same Si cluster structure without the water molecules (red). Also shown is the gap of the Si cluster in its relaxed, zero temperature structure (green). The arrow indicates the particular snapshot used to produce the electronic structure information in Figures 6 and 7 and Table 3.

The initial 0.17 ps of the FPMD simulation evolves under the influence of a velocity rescaling thermostat after which the temperature of the system reaches 300 K. At this point, the thermostat is removed and the simulation is allowed to evolve with constant total energy.[53]

We notice that the molecular structure of the solute is greatly perturbed during this simulation. This perturbation is caused by the nonequilibrium initial configuration that is used to start the simulation. We assume that the classical forces used to generate this initial configuration have some mismatch with the quantum mechanical forces present in the FPMD simulation. This mismatch greatly increases the average kinetic energy of the solute, as can be seen in Figure 5a (the average kinetic energy of the Si atoms in the solute, T_{Si}, is shown here converted to temperature units for comparison with the system temperature T_{tot}). We see that the solute is effectively equilibrated with the thermal bath of water molecules after 2 ps.

(50) Zhou, F.; Head, J. D. *J. Phys. Chem. B* **2000**, *104*, 9981−9986.
(51) Laurence, P. R.; Hillier, I. H. *Comput. Mater. Sci.* **2003**, *28*, 63−75.
(52) We have repeated our calculations of the activation energy using the B3LYP functional and obtained a value of 1.07 eV, which compares favorably with values reported by Laurence and Hillier of ~0.9 eV.[51]
(53) For the final 1.5 ps of the simulation, the time-step is increased to 3 au, while the fictitious electron mass was kept fixed at 276 au.

For such a small molecule, it is reasonable to predict that the impact of thermal fluctuations on the structure of $Si_5H_{10}O$(II) may have a marked impact on its optical properties. From previous work,[11,13,14] we know that the impact of deviations from tetrahedral coordination in Si clusters leads to large red shifts in the absorption gap. This is also observed in our finite temperature simulation. Taking snapshot structural configurations approximately every 0.1 ps from this simulation, we approximate the instantaneous absorption gap as the difference in total energy between the ground state and the triplet first excited state. This is shown in the black curve of Figure 5b. It is clear that variations in the absorption gap are highly correlated with the average kinetic energy (or instantaneous "temperature") of the Si atoms, shown in Figure 5a. The larger fluctuations in the absorption gap occur at higher temperatures, in the 2 ps equilibration phase of the simulation, where the corresponding structural fluctuations are largest, producing the greatest structural deviations. Once equilibrated, the fluctuations in the gap reach a steady standard deviation of ~0.3 eV. The equilibrated system displays a systematic red shift in the absorption gap of 0.7 eV from that of the solute in vacuo at 0 K.

X. Impact of Screening on Optical Absorption of Silicon Clusters

The observed 0.7 eV shift is not an effect due to polarization or dispersion from the surrounding solvent molecules. To verify this, we remove the water molecules from each structural configuration used previously and compute the absorption gap of the isolated $Si_5H_{10}O$(II) molecule. We find that the resulting unsolvated gaps [red curve in Figure 5a] follow the corresponding solvated gaps quite closely. We observe no systematic shift to the red or blue due to the presence of the solvent in the equilibrated phase of the simulation. This is a clear indication that the dominant factor influencing the absorption properties of the solute is the finite temperature of the system.

It is also interesting to note that even in the highly nonequilibrium phase of the simulation of the first 2 ps, structural variations remain the dominant factor in variations of the absorption gap. In this regime, the solvated and unsolvated gaps are practically the same, while fluctuating over a range of 1.5 eV.

The absence of a systematic solvent shift, due to screening, for the Si cluster in water is at variance with the solvent shifts of polar organic solutes in polar solvents, where an experimentally observed blue shift in the absorption gap is expected from screening arguments. Recent calculations by Bernasconi et al.[20] have shown that a solvent blue shift for acetone in water is resolvable from a relatively short FPMD simulation. This contrast with our results is interesting and may point to fundamental differences between organic and inorganic solutes in water.

XI. Electronic Structure

We analyze the electronic structure of the solvated system described in section IX to assess the validity of our approach to the calculation of absorption gaps, and to deduce why dielectric screening does not have a large impact on the optical properties. Figure 6 illustrates the charge density associated with several Kohn−Sham eigenstates near the Fermi level, for an isolated Si cluster (unsolvated), for the Si cluster surrounded by water (solvated), and for a configuration taken from a FPMD liquid water simulation at 300 K (water).

Table 3. Various DFT Estimates of the Absorption Gap for the $Si_5H_{10}O$(II) Molecule: In Its Vacuum, Zero Temperature Structure; at 300 K in Vacuo; and at 300 K in Water[a]

phase:	vacuum	vacuum	solvated
temp (K):	0	300	300
HOMO−LUMO	4.5	3.7	3.9
Δ*SCF* mixed	4.4	3.8	3.9
Δ*SCF* triplet	4.2	3.6	3.8
exchange-splitting	0.19	0.18	0.17

[a] The finite temperature estimates of the gap use the molecular structure of the snapshot considered in Figure 6. Also shown is the splitting between the mixed and triplet Δ*SCF* estimates of the gap. All energies are given in eV.

We examine first the states illustrated in Figure 6e−h. We notice that the HOMO of the solvated system [Figure 6e] is localized on the Si cluster solute. This localization of the HOMO is typical for each of the configurations examined in Figure 5. This is in contrast with, for example, the acetone−water system examined by Bernasconi et al.[20] In that work, the HOMO varied in its localization during the course of a FPMD simulation, at times reminiscent of the HOMO of the isolated acetone system, and at others more like the HOMO of water in the condensed phase.

The LUMO of the solvated system [Figure 6f] is entirely delocalized over the simulation cell. However, when we alter the occupancy of the Kohn−Sham eigenstates (as described in section IV) to produce the mixed or triplet first excited states, we notice that the HOMO* − the analogue of the LUMO in the occupied excited state − is localized on the solute. In comparison with the localized states of the unsolvated Si cluster shown in Figure 6a−d, only the LUMO of the solvated system differs significantly.

Our initial motivation for considering occupied excited state configurations was to capture the screening response of the solvent to variations in the solute charge density from its electronic ground state. We find that the physically different charge distributions associated with the LUMO and HOMO* of this solvated system are not significant for the various estimates of the absorption gap. We see from Table 3 that the HOMO−LUMO estimate is essentially the same as the Δ*SCF* mixed-state estimate.

Our use of the triplet excited state, for reasons of efficiency (section IV), is justified by the close physical resemblance of the charge densities of the HOMO* in each case. The splitting between the mixed and triplet Δ*SCF* absorption gaps can be associated with exchange effects local to the Si cluster, because the relevant gap states are localized on the cluster and the presence of water or the perturbation of the molecular structure has little effect on this splitting, which remains ~0.2 eV in all cases. As noted in section V, this estimate of the exchange-splitting is most likely an underestimate, and in a spin-restricted formalism it should be doubled. In our calculations, we are not justified in drawing such analogies because our Δ*SCF* calculations are spin-unrestricted.

However, the difference between the LUMO and HOMO* has important consequences for other physical quantities, such as the oscillator strength (*f*) for this transition. We find that for the HOMO−LUMO transition, $f = 0.05$, while for the transition from LUMO* to HOMO*, $f = 0.60$ (refer to Figure 2b for

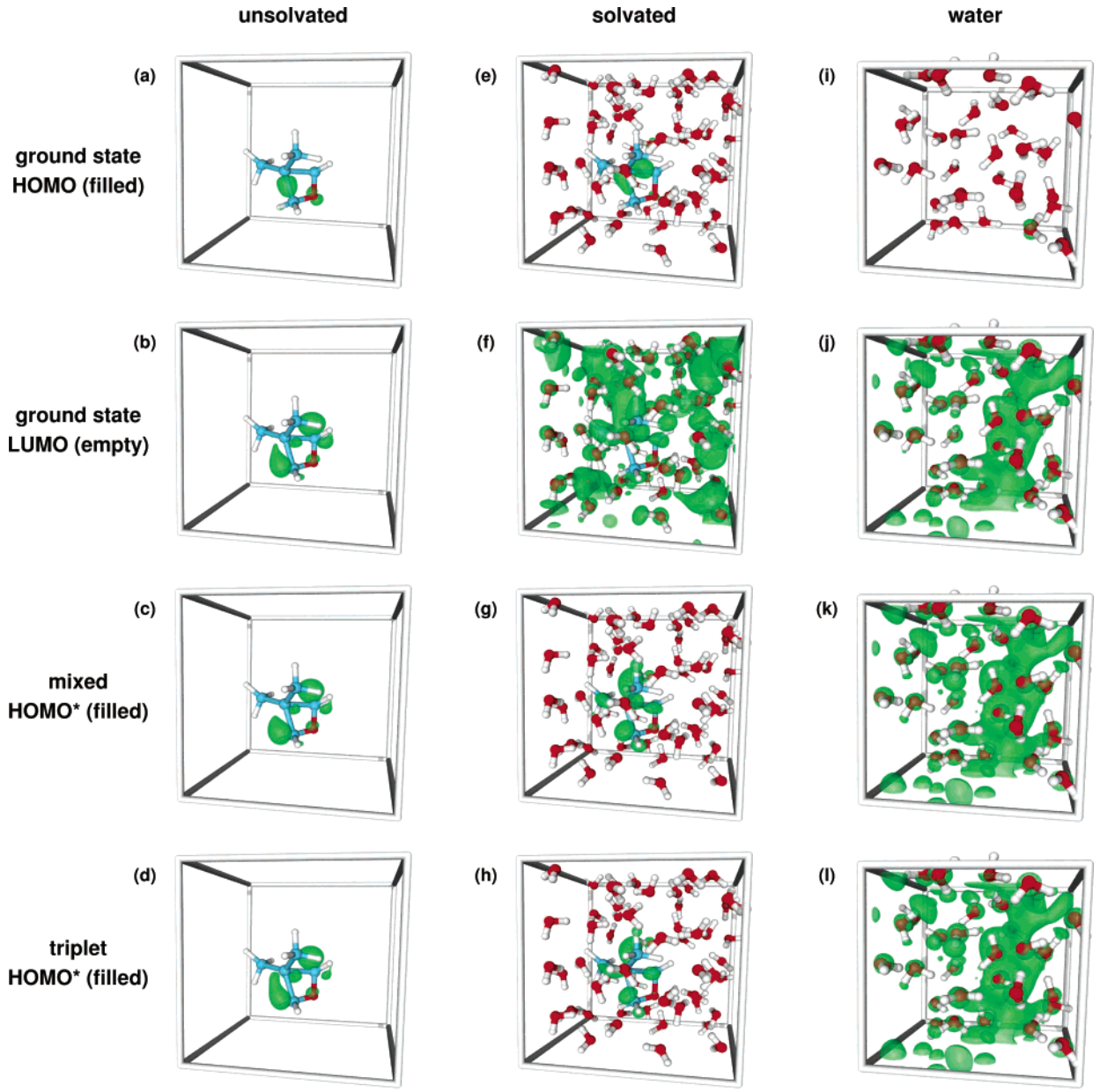

Figure 6. Electronic structure of various Kohn−Sham eigenstates near the Fermi level for a specific configuration chosen at the 2.5 ps point from the FPMD simulation of $Si_5H_{10}O$(II) in water outlined in Figure 5. The unsolvated systems (a)−(d) contain equivalent solute structures to the solvated systems (e)−(h), but have all water molecules removed. Also displayed in (i)−(l) are states near the Fermi level for a configuration taken from an FPMD simulation of water at 300 K. All charge density isosurfaces (green) contain 30% of the total charge of the given state. Atom colors are as indicated in Figure 3.

definitions of these states). Using the LUMO* is justified given its almost complete (99.8%) overlap with the HOMO of the ground state. This order of magnitude difference in f will have important consequences for calculated optical absorption.

The delocalization of the LUMO of the solvated system [Figure 5f] is reminiscent of the delocalized LUMO observed in previous DFT calculations of the electronic structure of liquid water.[54,55] An example of this LUMO of water is provided in Figure 6j. To interpret the origin of various states near the Fermi level of the solvated system, we compare its density of states (DOS), in Figure 7, to that of the unsolvated system and that of pure liquid water. The energy scale in this figure is shifted in such a way that the HOMO of the solvated system is at zero. Given that the HOMO and LUMO of the solvated system are qualitatively similar to the HOMO of the isolated solute and the LUMO of pure water, respectively, we choose to align these pairs of states for the sake of comparison. It is worth noting that this seemingly arbitrary alignment is consistent for other effective single-particle states. For example, the lowest valence s states of the oxygen atoms in each system are correctly aligned at around ~ -20 eV on this energy scale (this part of the DOS has been omitted for clarity in Figure 7). We also note that the isolated LUMO of liquid water, shown at ~2.5 eV in Figure 7c, is the subject of some controversy and may not reflect a physically observable transition.[20,56]

(54) Laasonen, K.; Sprik, M.; Parrinello, M. *J. Chem. Phys.* **1993**, *99*, 9080−9089.
(55) Boero, M.; Terakura, K.; Ikeshoji, T.; Liew, C. C.; Parrinello, M. *J. Chem. Phys.* **2001**, *115*, 2219−2227.
(56) Blumberger, J.; Bernasconi, L.; Tavernelli, I.; Vuilleumier, R.; Sprik, M. *J. Am. Chem. Soc.* **2004**, *126*, 3928−3938.

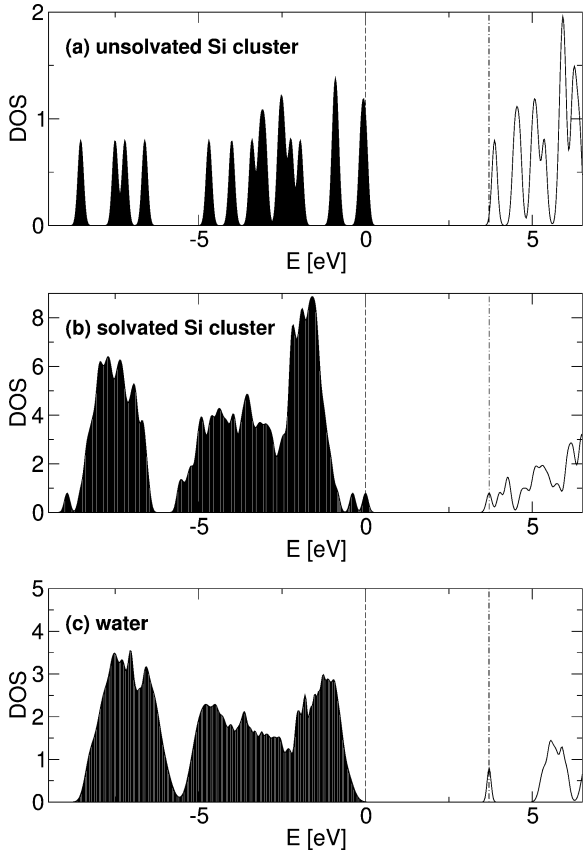

Figure 7. Density of states (DOS) of (a) the unsolvated Si cluster of Figure 6a; (b) the solvated Si cluster of Figure 6e; and (c) that of liquid water. The DOS of water was calculated by thermal averaging over 20 ps of a FPMD simulation of 32 water molecules at ambient pressure and 300 K. The average broadening of states for this simulation was 0.08 eV, which was then used to broaden the discrete spectra of (a) and (b). The energy scale in (b) is shifted to place the HOMO at zero (vertical dashed line). The shift in energy applied to (a) places the HOMO at zero also, while the shift applied to (c) aligns the LUMO with the LUMO of (b) (vertical dashed−dotted line). The oxygen s-states have been omitted, but lie at ~ -20 eV.

The DOS of the unsolvated Si cluster indicates another state quite close in energy to the LUMO of the solvated system, and, in fact, the LUMO+1 Kohn−Sham eigenstate of the solvated system resembles this unsolvated, localized, empty state. This is also true of the HOMO* of the mixed and triplet configurations. Therefore, we conclude that occupying the first excited state leads to a reordering of states near the Fermi level, such that the delocalized LUMO is replaced by a localized HOMO*. The preference for a localized HOMO* is due to the binding energy associated with the underlying charge distribution, which contains a "hole" (unoccupied LUMO*) localized on the Si cluster. To further illustrate this point, we note that for the states near the Fermi level in liquid water [Figure 6i−l], there is no significant difference between the charge densities of the LUMO and HOMO*. There is no localized state nearby in energy in the conduction band with which to swap, and also there is no localized "hole" to favor such a reordering of energy levels.

XII. Consequences for Experiment and Theory

There are several conclusions that experimentalists may draw from our computations. With regard to reactivity, we see that for absorption processes, the existence of the silanone group is very unlikely, given its low activation energy for reaction with water. Note that the existence of a photostable silanone in the presence of water, proposed by Zhou and Head,[50] is only relevant for emission processes. Also, other work[9] indicates that the significant red shift induced by this functional group may be reproduced by complete passivation with other types of oxygen-containing groups, such as hydroxyls and bridging oxygens.

We expect that the large red shift caused by thermal strain in our finite temperature simulations (Figure 5) may be more pronounced for this small prototypical cluster than it would be for a larger Si QD. For larger Si QDs, with more rigid surface reconstructions, we expect that finite temperature effects will play a smaller role in their impact on the absorption gap. This is further reinforced by the small temperature dependence of the lowest direct gap of bulk Si, which shifts to the red by only $\sim$0.05 eV upon increasing the temperature from 0 to 300 K.[57]

The lack of any screening impact on the absorption of such a small Si cluster with a relatively large dipole moment indicates that for larger Si QDs, this effect may also be negligible. The likelihood of complete passivation of the surface of a large Si QD with oxygen will significantly reduce the total dipole moment of such particles. Furthermore, the preference for oxygen-containing passivants which effectively preserve the local tetrahedral symmetry around each Si atom guarantees that the electronic states near the Fermi level are delocalized over the entire QD. Therefore, screening impacts are reduced, given that they are more likely to be limited to the surface region of the QD, not extending far into the core. However, in larger Si QDs, a smaller red shift due to thermal strain may permit the observation of small solvent shifts due to screening. This issue requires further investigation.

For theorists, it seems that simulating solvated Si QDs may not require large FPMD simulations that include water. Given that the screening impact is so small, there may be no advantage to including many solvation shells of water molecules in a simulation. On the other hand, analysis of ground-state structures and active vibrational modes at a given finite temperature may provide more useful information than large finite temperature simulations and thermodynamic averaging.

XIII. Conclusions

This is the first theoretical analysis of the impact of aqueous solvation on the optical properties of Si nanoparticles. While there have been many studies on the impact of polar solvents on the absorption properties of organic molecules, so far no investigation has been reported for inorganic solutes such as QDs. In our analysis, we considered three factors: chemical reactivity, thermal equilibration, and dielectric screening. Regarding chemical reactivity, we find that the silanone functional group is extremely reactive in the presence of water and is unlikely to exist in aqueous solution. We find that the bridging oxygen and hydroxide surface passivants are much more stable and therefore more probable sources of red shifts in the experimentally observed absorption spectra. At 300 K, we find that thermal fluctuations induce strain in the small silicon cluster examined here, and we estimate that this strain leads to a systematic red shift of $\sim$0.7 eV. Upon removing the screening

(57) Allen, P. B.; Cardona, M. *Phys. Rev. B* **1983**, *27*, 4760−4769.

impact of the surrounding water, we determine no noticeable impact of solvent polarization or dispersion on the optical absorption gap of this silicon cluster. Given the thermal stability of larger QDs, we conclude that chemically stable Si QDs will have robust optical properties in the presence of water, further justifying their use as stable and efficient optical tags in biological sensing applications.

Acknowledgment. We wish to thank F. Gygi, F. Reboredo, and T. Ogitsu for stimulating discussions. This work was performed under the auspices of the U.S. Department of Energy at the University of California/Lawrence Livermore National Laboratory under Contract No. W-7405-Eng-48.

JA048038P